EVALUATION OF INKJET PRINTED HEATERS ARRAY FOR CHEMO-RESISTIVE GAS SENSOR

[1]Vojtěch POVOLNÝ, [1]Alexandr LAPOSA, [1]Jiří KROUTIL, [1]Jan VOVES, [2]Petr ASHCHEULOV, [1]Pavel HAZDRA

[1]Faculty of Electrical Engineering, Czech Technical University in Prague, Prague, Czech Republic, EU, povolvoj@fel.cvut.cz

[2]Institute of Physics of the Czech Academy of Sciences, Prague, Czech Republic, EU

https://doi.org/10.37904/nanocon.2023.4770

Abstract

Heaters are an indispensable part of gas sensing platforms. It serves to heat the sensor, which increases the sensitivity of the active layer and helps in the desorption of the detected gas. The sensors are also heated to stabilize the parameters against the ambient temperature. For the fabrication of electronic circuits and devices including sensing platforms and heating structures is becoming increasingly popular to use flexible electronics. In particular, the use of inkjet printing technology allowing localized deposition of ink at low temperatures on a large area. Many kinds of inks such as conductive, semi-conductive, or dielectric can be used. In this research, we present the design preparation, simulation, fabrication, and characterization of the inkjet printed heaters. The structures are based on silver nanoparticle ink printed on a flexible substrate and are sintered with intense pulsed light. The printed heaters consist of connection pads, interconnection pathways, and heater patterns. Two types of heater patterns were designed (meander and dual-spiral type). Both of the prepared patterns were simulated in Ansys simulation software to obtain the heat distribution. The microheaters were printed on a polyethylene terephthalate (PET) substrate and characterized with a thermal imaging camera. Based on the results obtained from these measurements, a calibration plot was created.

Keywords: Inkjet, gas sensor array, PET, IPL, microheater

1. INTRODUCTION

Inkjet printing is a kind of additive manufacturing technology, which is very popular in a wide range of academic and industrial fields. It allows the production of electronic structures with a fully additive process by drop-on-demand or on-demand material deposition technology. Compared to the conventional electronic production process Inkjet printing does not require to be placed in clean rooms. Low manufacturing costs, a wide range of flexible and rigid substrates, a low-temperature production process, and ease of use are the key advantages of this technology [1]. A variety of electronic devices, such as all-polymer transistors [2], [3], light emitting diode (PLED) [4], [5], nanoparticle Micro Electro Mechanical Systems [6], or chemo-resistive gas sensors [7] have been made with inkjet printing.

In many different branches of electronics development, a certain element or area must be heated to achieve the expected performance or correct response. For example, many biosensors or gas sensors require high temperature to achieve high selectivity and sensitivity [8], [9]. For this reason, it is desirable to design small, low-cost heating elements with low power consumption, which could be easily integrated as close as possible to the area, where temperature control is required [10].

In this work, we report the preparation of two types of an Inkjet printed heater matrix on a flexible substrate. We discuss the heat propagation of the structures, the reached temperature for different current levels obtained from thermal measurements, and the results obtained from the simulation.

2. MATERIALS AND METHODS

2.1. Heater array fabrication

The prepared heater array was designed as a part of the multilayer sensor array, see **Figure 1**. The evaluation and preparation of interdigital structure and dielectric mask were presented in [11]. The structures were printed with material inkjet printer Fujifilm Dimatix 2831 and cartridge DMC-11610 (16 nozzles, 10 pl drop volume) and the design of the platform was prepared with the CleWin5 layout editor (Wieweb software, Netherland). The heater layout consists of three basic parts – contact pads, interconnections, and heating structure, see **Figure 2A**. The connector pads are designed to be simply connected with a flexible tip or to be mounted into an Amphenol Clincher flex connector. The heated area is 2 mm x 2 mm. Two types of heater patterns were designed for printing – A) meander and B) dual spiral type. Each of the mentioned types was printed in a matrix of four interconnected heating structures. The printed structures and the layouts with dimensions can be seen in **Figure 2B, C**.

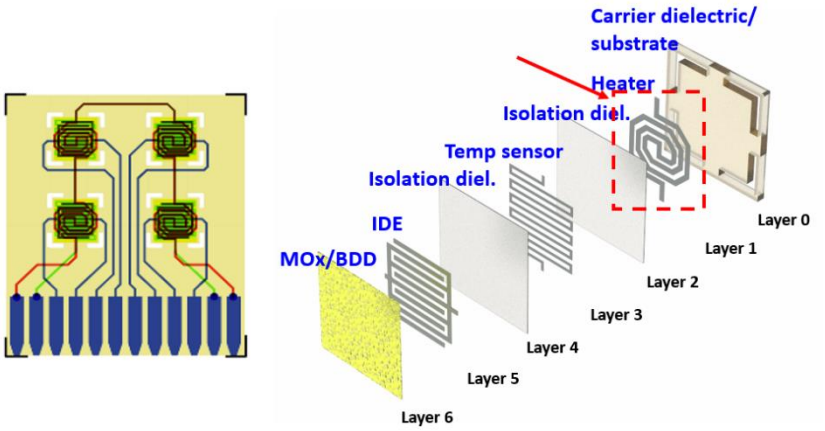

Figure 1 Platform of printed interdigital sensor array: A) Complete sensor array with all layers, B) Exploded schema of the sensor array.

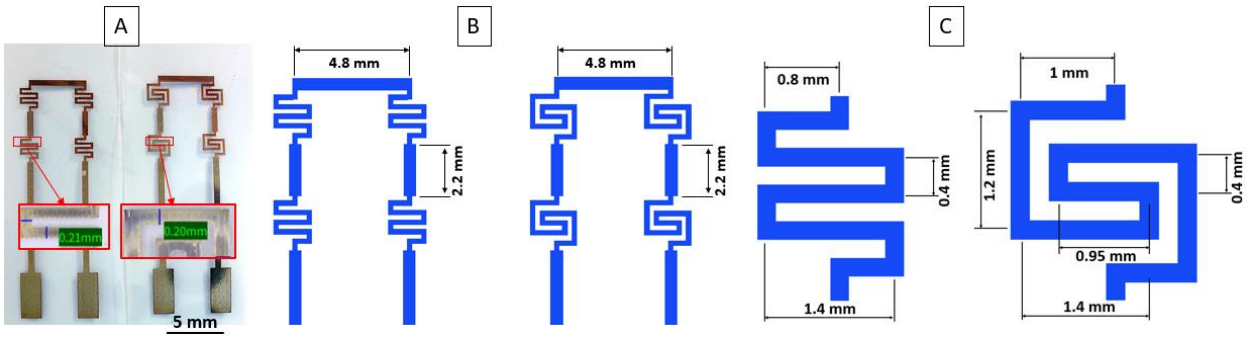

Figure 2 Printed heaters on flexible PET substrate: A) Meander and double-spiral type heater structures printed with silver ink, B) Matrix of meander and double-spiral heater structures, C) Detail layout of the meander and double-spiral heater structures.

2.2. Substrate and ink

The presented structures were printed with the silver nanoparticle ink ANP Silverjet DGP-40LT-15C having particle size <50 nm, solid content 35 %, and resistivity 11 μΩ·cm. This ink was printed on 140 μm thick polyethylene terephthalate (PET) substrate from Mitsubishi NoveleTM IJ-220 by Novacentrix which is a mesoporous flexible and transparent substrate. It is suitable for low-temperature and low-cost inkjet printed applications [11]. Typical parameters of PET substrates are listed in **Table 1**. Technical parameters of the selected substrate are listed in **Table 2**.

The structures were printed on the substrate heated to 40 °C with a DMC 11610 cartridge, heated to 35 °C. While printing, the resolution was set to 1016 dpi at 2 kHz jetting frequency. After 24 hours of drying at room temperature, the structures were sintered with the high-intensity pulse light (IPL) system (Xenon X-1100 by

Xenon corporation, USA) with up to 9 J·cm^{-2} radiant energy per pulse, broad-spectrum light. Flash parameters were set at 300 µs and 200 J, and 3 flashes were applied to each structure.

Table 1 Typical properties of PET substrates

Property	Tensile strength (MPa)	Flexibility	Dimensional stability	Dielectric strength (kV/mm)	Max operating temperature (°C)	Chemical resistance	Moisture absorption (%)	Cost
Polyethylene terephthalate (PET)	60 – 85 *	Excellent	Good	20 – 50 *	100 – 140 *	Very good	0.10	Low

* – According to type

Table 2 Parameters of Mitsubishi Novele IJ-220 PET foil

Basis Weight (g·m^2)	Thickness (µm)	Volume conductivity (%)	Smoothness (Sec)
175±10	140±12	< 22	> 1000

2.3. Simulation and thermograms

The heat distribution of the designed layouts was investigated by Ansys 2021 simulation software (Ansys, Inc., Pennsylvania, USA). The simulated structures were designed with the dimensions as are shown in **Figure 2**. For the simulation, the PET substrate was defined with a thermal conductivity of 0.3 W·(m·K)$^{-1}$. For the modeled conductive structures, the silver material with a specific resistivity of 11 µΩ·cm was defined. By simulating the designed structures, we determine the heat propagation through the substrate in the vicinity of the heating part of the structures and any differences in propagation between the selected types for defined current through the structure.

The thermal measurements were performed with the thermal camera Optris XI 400. Before starting the measurements, calibration was done to ensure the measured temperature matched the ambient temperature. The control software allows both single-point and area temperature measurements. Both options were used during the measurement of the printed structures. As can be seen in the following thermograms, the printed structures appear significantly colder than the surroundings. This is due to the shiny surface of the silver and its emissivity, which in this form is 0.02. However, with this value set, it was not possible to measure structures with a result corresponding to reality. In this case, we assume that the temperature of the substrate right next to the heated structure has the same temperature as the structure itself, and this was recorded for further evaluation.

3. RESULTS AND DISCUSSIONS

3.1. PET – Printed structures

The heater structures were printed in two layers which is equivalent to a thickness of 1 µm, according to the previously reported measurements [11]. Before thermal measurements, it was verified that the structures were not interrupted by optical spectroscopy and electrical measurements.

The prepared structures were mounted into the 3D printed holder with a hole under the heating structure. This ensures that the foil remains flat and the heating part of the structure does not cool by contact with the underlay. The measuring setup and printed sample are shown in **Figure 3A, B**. The structures were contacted with flexible tips on contact pads, and a current from 10 mA to 150 mA was gradually applied to the structures in 10 mA steps. Before measurements, the printed structures were additionally annealed with a current of 120 mA for 1 min. **Figure 3C, D** shows thermograms of both types of printed heater structures at the temperature of 100 °C. It can be seen that the dual-spiral structure has about 12 % larger area heated to the maximum temperature than the meander structure. **Figure 4** shows thermograms of heating structures at passing currents of 60 mA, 80 mA, and 100 mA. For the current of 60 mA and 80 mA, the area and temperature to

which both structures are heated are almost identical for both types (62 °C for the meander and 64 °C for the dual-spiral type at 80 mA). However, from the current of 80 mA, the heat spreading to the center starts to be significant. For the passing current of 100 mA, there is a more significant difference in the heated area between the heater structures. On the other hand, it can be seen that the meander structure (**Figure 4B**) spreads the heat more into the center of the matrix than the dual-spiral type. Moreover, it can be seen that the area with the highest temperature is slightly misalignment from the center of the heating structure due to heat sharing between each heater and the cooling effect outside the heating platform. When the substrate with the printed structures were unmounted from the holder it was found that the high temperature caused deformation of the PET foil. Therefore, for temperatures above 100 °C, it will be necessary to use another material with higher temperature endurance (for example polyimide).

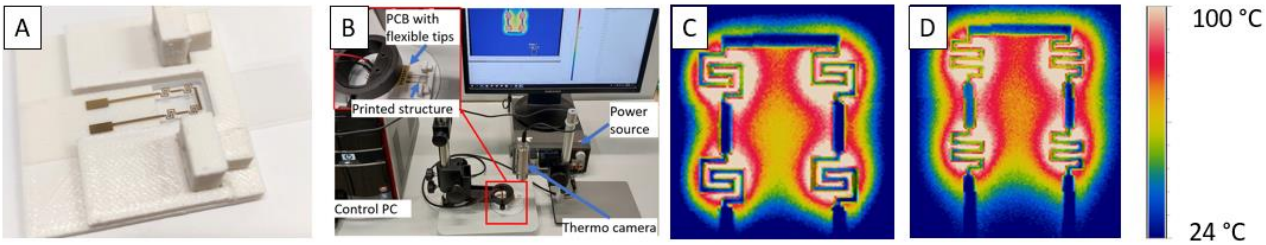

Figure 3 A) PET foil with inkjet printed heater structure mounted in the 3D printed holder; B) the measuring setup; thermograms of dual-spiral B) and meander C) matrix heater structures at the temperature of 100 °C.

Figure 5A shows the measured temperatures and simulated values for both structures. There are two pairs of simulated curves in the graph which differ in the thickness of the silver layers. For the first pair, represented by Model 1 in the plot, the set thickness was measured with a profilometer. It can be noticed that as the current increases, the temperature increases exponentially. From this result, we assume that the thickness of the silver layer has to be greater. Because the used substrate is mesoporous, the printed ink soaks up into the substrate and it is difficult to measure the real profile of the printed layer. For the second pair, represented by Model 2 in the plot, the thickness was fitted to correspond to the real measured temperatures. With this modification, we can specify the thickness of the silver layer on the PET substrate. The simulation results of Model 2 correspond to the measured temperatures of the printed structures and the corrected thickness of the silver layer was observed to be 4 µm.

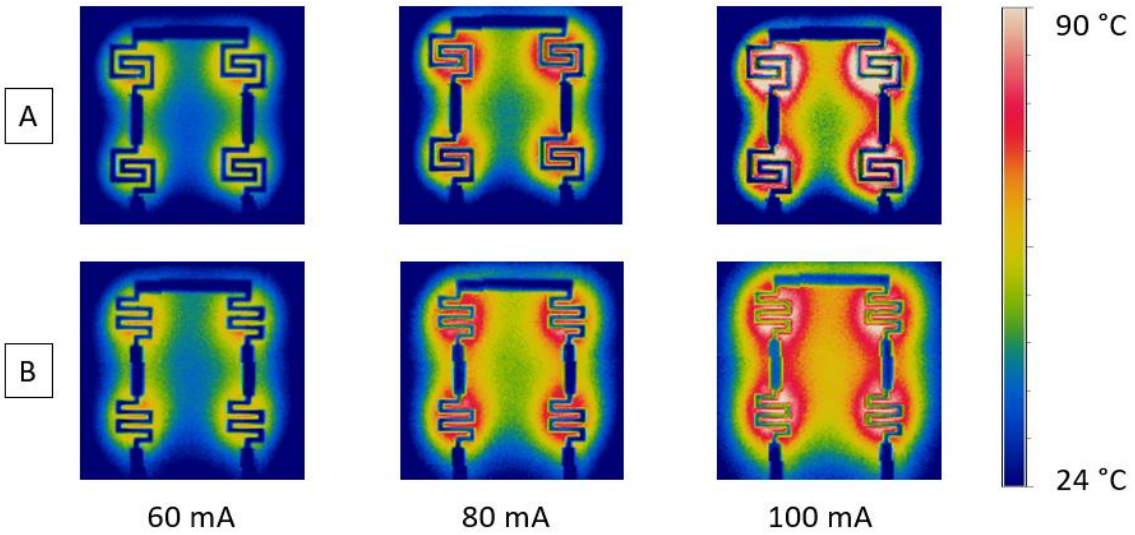

Figure 4 Thermograms of A) dual-spiral and B) meander heating structures at a passing current of 60 mA, 80 mA, and 100 mA.

In addition, the time required to heat the structure from ambient temperature to 100 °C was measured. The dual-spiral type reached the desired temperature in 55 seconds and the meander type in 57 seconds, respectively. Moreover, the resistance of the structures at selected temperatures was calculated. It can be noticed that due to the more complex design of the dual-spiral structure it has a 4 Ω higher resistance than the meander structure, see **Figure 5B**.

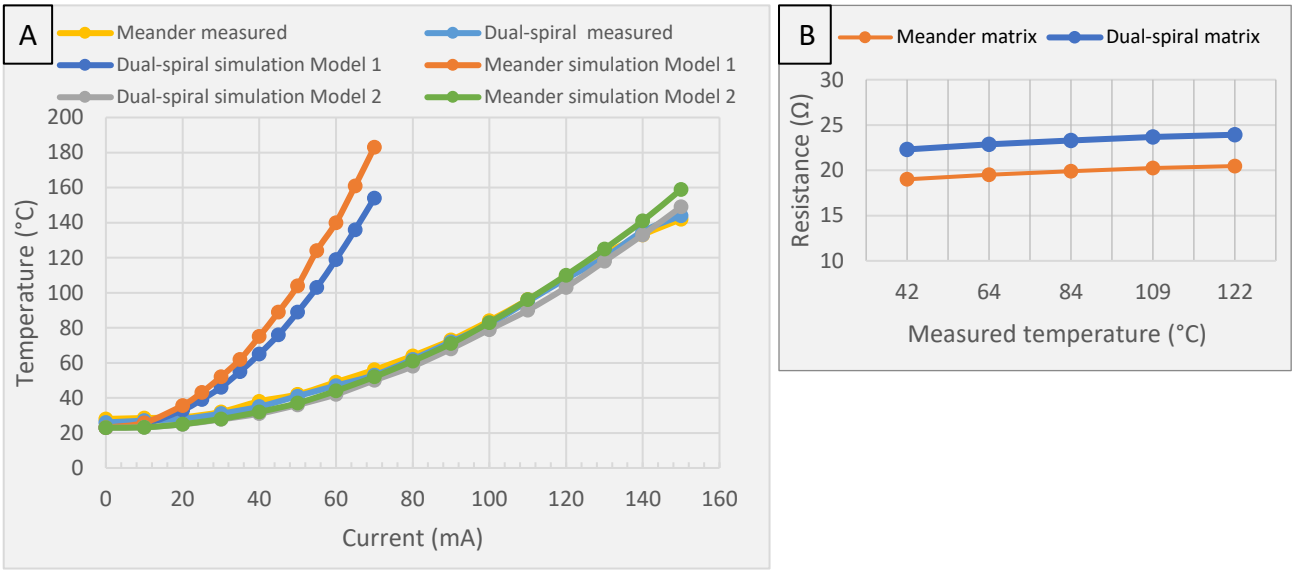

Figure 5 A) Graph of the simulated and measured temperatures for the different values of passing current, B) Resistance dependency on measured temperature of printed heater structures.

3.2. Simulation

In **Figure 6**, simulated heater structures can be seen. The simulated thermograms show the structures at the maximal temperature of 100 °C. It can be seen an uneven heating of the upper structures, which is not observed in printed structures. Regarding the temperature profile and heat propagation into the center of the matrix and its surroundings, the measured data correspond to the simulated results. The simulations confirm the misalignment of the preheated area from the center of the heating structures as well.

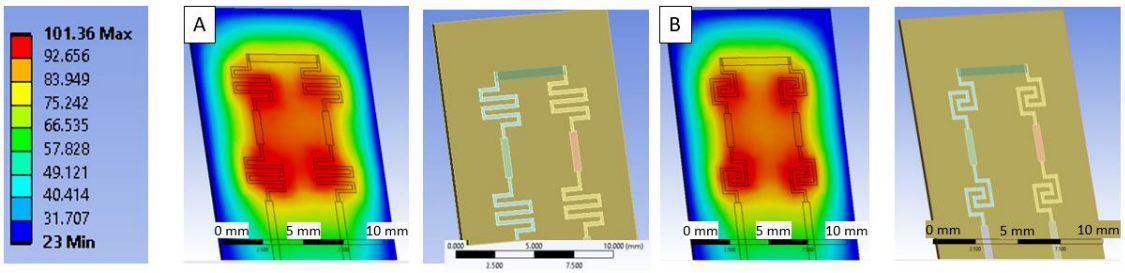

Figure 6 Simulated structures and thermograms of A) meander and B) dual-spiral heater structure matrix in Ansys simulation software

4. CONCLUSION

In this work, the two types of heaters were fabricated. Meander type and dual-spiral type heaters were printed on PET flexible and transparent substrate by inkjet printing of silver nanoparticle ink. Investigations of the heating of selected structures have shown that they can reach temperatures higher than 100 °C, which is sufficient for the flexible gas sensor requirements. Specifically, the meander structure reached 142 °C and the dual-spiral structure reached 144 °C. Both of the heater structures exhibit a similar result, however, the dual-

spiral type shows a larger area heated to the maximum temperature around the heating structure at the same current passing, which was also confirmed by simulation. From this perspective, the dual-spiral type is more suitable to be used for further heating in a multilayer sensor platform. However, for temperatures higher than 100 °C, a material with a higher heat endurance will be required to avoid high-temperature damage. Moreover, from the results of the simulation and measured temperature, the thickness of silver printed layers was specified.

ACKNOWLEDGEMENTS

This work was supported by the Czech Science Foundation grant No. 22-04533S and by the Czech Technical University Student Grant No. SGS23/182/OHK3/3T/13.

REFERENCES

[1] B. J., KANG; C. K., LEE and J. H. OH. All-inkjet-printed electrical components and circuit fabrication on a plastic substrate. *Microelectron. Eng.* 2012. Available from: https://doi.org/10.1016/j.mee.2012.03.032.

[2] H. SIRRINGHAUS *et al.* High-resolution inkjet printing of all-polymer transistor circuits. *Science (80-.).*, 2000. Available from: https://doi.org/10.1126/science.290.5499.2123.

[3] T. KAWASE; H. SIRRINGHAUS; R. H. FRIEND and T. SHIMODA. “Inkjet printed via-hole interconnections and resistors for all-polymer transistor circuits.” *Adv. Mater.* 2001. Available from: https://doi.org/10.1002/1521-4095(200111)13:21<1601::AID-ADMA1601>3.0.CO;2-X.

[4] T. R., HEBNER; C. C., WU; D., MARCY; M. H., LU and J. C., STURM. “Ink-jet printing of doped polymers for organic light emitting devices.” *Appl. Phys. Lett.* 1998. Available from: https://doi.org/10.1063/1.120807.

[5] Y. YANG; S. C. CHANG; J. BHARATHAN and J. LIU. “Organic/polymeric electroluminescent devices processed by hybrid ink-jet printing.” *J. Mater. Sci. Mater. Electron.*. 2000. Available from: https://doi.org/10.1023/A:1008968511133.

[6] S. B., FULLER; E. J., WILHELM and J. M., JACOBSON. “Ink-jet printed nanoparticle microelectromechanical systems.” *J. Microelectromechanical Syst.* 2002. Available from: https://doi.org/10.1109/84.982863.

[7] L. GE *et al.*. “A fully inkjet-printed disposable gas sensor matrix with molecularly imprinted gas-selective materials.” *npj Flex. Electron.* Jun. 2022, vol. 6, no. 1, p. 40. Available from: https://doi.org/10.1038/s41528-022-00168-6.

[8] A., BISCOTTI; R., LAZZARINI; G., VIRGILLI; F., NGATCHA; A., VALISI and M., ROSSI. “Optimizing a portable biosensor system for bacterial detection in milk based mix for ice cream.” *Sens. Bio-Sensing Res.* Apr. 2018, vol. 18, pp. 1–6. Available from: https://doi.org/10.1016/j.sbsr.2018.02.002.

[9] A. C., CATTO *et al.* “Local Structure and Surface Properties of Co x Zn 1– x O Thin Films for Ozone Gas Sensing.” *ACS Appl. Mater. Interfaces*. Oct. 2016, vol. 8, no. 39, pp. 26066–26072. Available from: https://doi.org/10.1021/acsami.6b08589.

[10] A. FALCO *et al.* “Printed and Flexible Microheaters Based on Carbon Nanotubes.” *Nanomaterials*. Sep. 2020, vol. 10, no. 9, p. 1879. Available from: https://doi.org/10.3390/nano10091879.

[11] V., POVOLNY; A., LAPOSA, J.; KROUTIL, J.; VOVES, M., DAVYDOVA, and P., HAZDRA. “Evaluation of printed interdigital electrodes array for chemo-resistive gas sensor application.” In *Proceedings 14th International Conference on Nanomaterials - Research & Application*, Ostrava: Tanger Ltd., 2022, pp. 45–51. Available from: https://doi.org/10.37904/nanocon.2022.4588.